

EPJ B

Condensed Matter
and Complex Systems

EPJ.org
your physics journal

Eur. Phys. J. B (2013) 86: 486

DOI: [10.1140/epjb/e2013-40893-4](https://doi.org/10.1140/epjb/e2013-40893-4)

Propagation in one-dimensional crystals with positional and compositional disorder

A. Maurel and P.A. Martin

edp sciences



 Springer

Propagation in one-dimensional crystals with positional and compositional disorder

A. Maurel^{1,a} and P.A. Martin²

¹ Institut Langevin, 1 rue Jussieu, 75005 Paris, France

² Department of Applied Mathematics and Statistics, Colorado School of Mines, Golden, CO 80401, USA

Received 29 July 2013 / Received in final form 5 October 2013

Published online 28 November 2013 – © EDP Sciences, Società Italiana di Fisica, Springer-Verlag 2013

Abstract. Propagation in perturbed one-dimensional phononic or photonic crystals, with both compositional and positional disorder, is considered. The coherent potential approximation is used to obtain the band structure and the Floquet normal form of the periodic-on-average perturbed crystal, which is modified differently with respect to the two kinds of disorder. For finite size crystals, the transmission amplitude is calculated and compared to direct numerical simulations and to an estimate based on localization length. The transmission spectrum is found to be better described using the full expression of the Floquet modes of the disordered, but periodic on average, medium.

1 Introduction

Disordered photonic and phononic crystals have experienced an increasing interest in recent years because of their potential applications to acoustic filters [1,2], the control of vibration isolation [3], noise suppression, and the possibility of building new transducers [4]; for a review see [5]. It is thus of interest to understand which properties of such structures are sensitive to inherent imperfections in their design and which are not.

Disorder is known to produce localization. In quantum mechanics, localization is discussed in terms of the Lyapunov exponent and spatially localized solutions of the Schrödinger equation. These localized modes always appear in an infinite disordered medium, and they can appear in a disordered medium of finite size. In classical waves, it is usual to characterize the medium in terms of an effective medium. One finds that the dispersion relation $K(\omega)$ departs from the dispersion relation $k(\omega)$ in the absence of disorder, and the imaginary part of the effective wavenumber K equals the inverse of the localization length in most cases. In the case where the unperturbed medium is free space, the imaginary part of the effective wavenumber K is only due to the introduced disorder. In the case of photonic or phononic crystals, the band structure of the unperturbed medium is more complicated, with a wavenumber Q of the Bloch Floquet mode being either purely real (pass band) or purely imaginary (stop band). Thus, the modification of the band structure when disorder is introduced is more involved [6,7]. Recently,

some unexpected behaviors have been observed, such as the suppression of localization in layered left- and right-handed structures perturbed in the optical indices [8,9] and the conversion of stop bands into pass bands in opal-type systems [10].

In this paper, we consider the propagation of a wave described by the wavefield $u(x)$ in a one-dimensional phononic/photonic crystal made of point scatterers (Kronig-Penney system) [11,12]. The wavefield u satisfies

$$u''(x) + k^2 u(x) = 2k \sum_n V_n \delta(x - x_n) u(x), \quad (1)$$

with V_n being dimensionless and purely real to ensure energy conservation. This model has a range of applications including low frequency propagation of guided waves [13–16] and propagation in crystal lattices [17,18]. The perfect periodic situation occurs when $x_n = nd$ and $V_n = V$. Here we consider the case of both compositional disorder and positional disorder, namely

$$\begin{aligned} V_n &= (1 + \xi_n)V, & \text{with } |\xi_n| &\leq \xi/2, \\ x_n &= (n + \epsilon_n)d, & \text{with } |\epsilon_n| &\leq \epsilon/2. \end{aligned}$$

In our derivation, we are restricted to the cases where $\epsilon < d$. This is of importance since we can define a unit cell, say $[(n - 1/2)d; (n + 1/2)d]$ that contains a single scatterer for any realization of the disorder. This means that the case of scatterers randomly distributed with all space available is inaccessible in our study: our reference configuration is the perfect periodic configuration.

We apply the coherent potential approximation (CPA) to derive the form of the Floquet normal form of the

^a e-mail: agnes.maurel@espci.fr

perturbed phononic crystal, assuming that the effective medium behaves as a periodic-on-average medium. This means that the full characterization of the wave is obtained, beyond the determination of the effective wavenumber K only. Namely, we find

$$v(x) = f(x)e^{iKx} + g(x)e^{-iKx}, \quad (2)$$

with $g(x) = f(d-x)$, $f(x)$ a d -periodic function,

$$f(x) = e^{i(k-K)x} + \mathcal{B}e^{-i(k+K)x},$$

and

$$\mathcal{B} = \frac{e^{i(k-K)d} - 1 - iV[1 - \text{sinc}(\epsilon kd)]}{1 - e^{-i(k+K)d} - iV[1 - \text{sinc}(\epsilon kd)]}$$

with $\text{sinc } x = (\sin x)/x$. In equation (2), $v = u$ in the perfect periodic case and $v = \langle u \rangle$ refers to the wavefield averaged over all realizations of disorder when the perturbed periodic case is considered.

The CPA calculation is performed for an infinite system at second order in both ϵ and ξ . This allows us to see how the band structure is modified differently with respect to the two kinds of disorder. The result is compared with the Lyapunov exponent calculated in [19] using a Hamiltonian map approach (a discrepancy is found in the result on the effect of the compositional disorder).

For comparison with our direct numerical calculations, slabs of finite size (N point scatterers, say) are considered. Assuming that the decomposition into right- and left-going Floquet normal modes is still valid in finite size system, we derive the transmission amplitude T_N (see Eq. (37)), that accounts for the internal reflections in the slab. Comparisons of the transmission amplitude $|T_N|_{\text{CPA}}$ obtained using our CPA approach and numerical results show good agreement, except near the band edges. When compared to an usual estimate of the transmission coefficient, or localization factor, $|T_N|_{\text{loc}} = e^{-Nd/L_{\text{loc}}}$, our prediction appears to be more precise because it accounts for the finite size of the slab.

2 Coherent potential approximation in a perturbed phononic crystal

We apply the coherent potential approximation (CPA), initially developed in terms of the effective Green function in the context of electronic transport in disordered alloys [20] and adapted to the problem of propagation in perturbed periodic media [21].

In the CPA, the scattering matrix of a unit cell embedded in an effective medium is considered (Fig. 1). When the unit cell is identical to the cells described by the effective medium, the scattering matrix is required to be the identity, and this allows us to derive the properties of the effective medium. This approach has been extensively used in periodic media (see e.g., [22,23]) and in random media (e.g., [24]).

In this paper, we adapt the CPA to characterize the normal Floquet mode to the case of a disordered system,

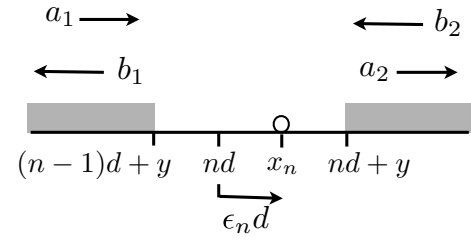


Fig. 1. Configuration used in the CPA approach. An isolated cell $(n-1)d + y < x < nd + y$ is embedded in a host medium. Inside the cell, there is a single scatterer located at x_n .

periodic on average. To do that, the perfect periodic case is used. We first derive the system of equations (10) that will be used in both perfect and perturbed periodic cases. We consider a unit cell containing a single scatterer. The cell is embedded in an effective periodic medium (perfectly periodic or periodic on average) and the medium is characterized by a Floquet mode with normal form for the right-going wave $f(x)e^{iKx}$, where $f(x)$ is a d -periodic function. The left-going wave is $g(x)e^{-iKx}$ with $g(x) = f(d-x)$.

2.1 Scattering matrix of a unit cell embedded in an effective medium

The scattering matrix of the cell is written

$$\begin{pmatrix} b_1 \\ a_2 \end{pmatrix} = \mathcal{S} \begin{pmatrix} a_1 \\ b_2 \end{pmatrix} \quad (3)$$

with

$$\mathcal{S} = \begin{pmatrix} r & \tilde{t} \\ t & \tilde{r} \end{pmatrix}. \quad (4)$$

The solution can be written as

$$v(x) = \begin{cases} a_1 f(x)e^{iKx} + b_1 g(x)e^{-iKx}, & x < (n-1)d + y, \\ A_1 e^{ikx} + B_1 e^{-ikx}, & (n-1)d + y \leq x < x_n, \\ A_2 e^{ikx} + B_2 e^{-ikx}, & x_n \leq x < nd + y, \\ a_2 f(x)e^{iKx} + b_2 g(x)e^{-iKx}, & x \geq nd + y, \end{cases} \quad (5)$$

with $\epsilon d/2 < y < (1-\epsilon/2)d$. This ensures that the scatterer remains inside the unit cell for any value of $x_n = (n + \epsilon_n)d$, $|\epsilon_n| \leq \epsilon/2$, and does not reach the interfaces of the cell. Thus, the boundary conditions to be applied at each interface of the cell are the continuity of the field v and its first derivative v' . At the scatterer position $x = x_n$ inside the cell, v satisfies

$$\begin{aligned} v(x_n^-) &= v(x_n^+), \\ v'(x_n^+) - v'(x_n^-) &= 2kV_n v(x_n), \end{aligned}$$

with $V_n = V(1 + \xi_n)$. The calculations are straightforward (some technical derivations are collected in the Appendix). An important immediate result is obtained: the scattering matrix is not expected to depend on the y -value. Indeed, the interfaces $x = (n-1)d + y$ and $nd + y$ are fictitious

and moving them within the above mentioned limits on y leaves the problem unchanged. As a consequence, the form of the function $f(x)$ can be deduced: to do that, it is sufficient to consider the transfer matrix \mathbb{T}_1 at the first interface $x = (n - 1)d + y$, written as

$$\begin{pmatrix} A_1 e^{iknd} \\ B_1 e^{-iknd} \end{pmatrix} = \mathbb{T}_1 \begin{pmatrix} a_1 e^{iKnd} \\ b_1 e^{-iKnd} \end{pmatrix}, \quad (6)$$

with

$$\mathbb{T}_1 = \begin{pmatrix} F_+(y)e^{i(k-K)d} & F_-(d-y) \\ F_-(y)e^{-i(K+k)d} & F_+(d-y) \end{pmatrix}, \quad (7)$$

where we have defined

$$F_{\pm}(y) = \pm[f'(y) + i(K \pm k)f(y)]e^{i(K \mp k)y}/(2ik) \quad (8)$$

(and we have used $g(y) = f(d - y)$). Because \mathbb{T}_1 cannot depend on y , F_{\pm} have to be constant. Without loss of generality, we choose $F_+ = 1$ and $F_- = \mathcal{B}$, with \mathcal{B} a constant to be determined. The differential system, equation (8), becomes

$$\begin{aligned} [f'(y) + i(K + k)f(y)]e^{i(K-k)y} &= 2ik, \\ [f'(y) + i(K - k)f(y)]e^{i(K+k)y} &= -2ik\mathcal{B}, \end{aligned}$$

which we integrate to obtain

$$f(y) = e^{i(k-K)y} + \mathcal{B}e^{-i(k+K)y} \quad \text{for } 0 < y < d. \quad (9)$$

This result is of importance since it reduces the determination of the function f to the determination of the constant \mathcal{B} only. Also, it is consistent to find that the function f restores the behavior of the wave within a unit cell: the wave is described by a combination of Floquet modes $f(x)e^{iKx}$ and $g(x)e^{-iKx}$, which, from (9) (and $g(y) = f(d - y)$), turns out to be a combination of a right-going wave e^{ikx} and a left-going wave e^{-ikx} propagating in free space as expected.

Using equation (9), it is straightforward to derive the scattering matrix (see the Appendix). We report the results (r, t) , expressed as the solutions of the system below

$$\begin{cases} [1 + iV_n + iV_n\mathcal{B}e^{-2i\epsilon_n kd}]t - \mathcal{B}re^{-2iKnd} = e^{i(k-K)d}, \\ [-iV_n e^{2i\epsilon_n kd} + \mathcal{B}(1 - iV_n)]t - re^{-2iKnd} = \mathcal{B}e^{-i(k+K)d}. \end{cases} \quad (10)$$

This system is a pair of equations involving four unknowns, r , t , $\mathcal{B}(\epsilon, \xi)$ and $K(\epsilon, \xi)$, all dependent on ϵ and ξ . In addition to the explicit dependence on ϵ_n and ξ_n in equation (10), only t and r depend on ϵ_n and ξ_n . We also report the expression of $t = \hat{t}$ (see Eq. (4)), solution of (10),

$$\begin{aligned} t(\epsilon, \xi; \epsilon_n, \xi_n) &= \frac{1 - \mathcal{B}^2 e^{-2ikd}}{\Omega} e^{i(k-K)d}, \\ \Omega &= (1 + iV_n) + 2iV_n\mathcal{B} \cos(2\epsilon_n kd) - \mathcal{B}^2(1 - iV_n), \end{aligned} \quad (11)$$

which will be used in the following.

2.2 The perfectly periodic case

We denote here

$$r_0(\epsilon_n, \xi_n) \equiv r(0, 0; \epsilon_n, \xi_n), \quad t_0(\epsilon_n, \xi_n) \equiv t(0, 0; \epsilon_n, \xi_n),$$

the reflection and transmission amplitudes when the host medium is perfectly periodic. Also, we denote

$$\mathcal{B}_0 \equiv \mathcal{B}(\epsilon = 0, \xi = 0), \quad Q \equiv K(\epsilon = 0, \xi = 0),$$

the corresponding Floquet normal mode and wavenumber. The CPA predicts that the unit cell is transparent for the wave propagating in the host medium when it is identical to the cells forming the host medium. The unit cells in the perfectly periodic medium are composed of identical point scatterers located at md ($\epsilon_m = 0$) and with potential strength $V_m = V$, ($\xi_m = 0$). We deduce that

$$r_0(0, 0) = 0 \quad \text{and} \quad t_0(0, 0) = 1, \quad (12)$$

which gives, from (10),

$$\begin{cases} 1 + iV + iV\mathcal{B}_0 = e^{i(k-Q)d}, \\ -iV + \mathcal{B}_0(1 - iV) = \mathcal{B}_0 e^{-i(k+Q)d}. \end{cases} \quad (13)$$

Eliminating \mathcal{B}_0 gives the dispersion relation for the Floquet mode as the condition of solvability, namely,

$$\cos Qd = \cos kd + V \sin kd. \quad (14)$$

We also find that

$$\mathcal{B}_0 = \frac{e^{i(k-Q)d} - 1}{1 - e^{-i(k+Q)d}}. \quad (15)$$

The normal form of the Floquet mode in the perfect periodic case is given by the Floquet wavenumber Q and the function $f(x)$ in equation (9), with $\mathcal{B} = \mathcal{B}_0$.

Although we only need here to consider the scattering matrix for $\epsilon_n = \xi_n = 0$, it will be useful for the following to derive the expansion of $t_0(\epsilon_n, \xi_n)$ at first order in ϵ_n and ξ_n . From equation (11), we obtain

$$\begin{aligned} t_0(\epsilon_n, \xi_n) &= 1 - iV \frac{(1 + \mathcal{B}_0)^2 e^{i(K-k)d}}{1 - \mathcal{B}_0^2 e^{-2ikd}} \xi_n + O(\epsilon_n^2, \xi_n^2) \\ &= 1 - iV \frac{\sin kd}{\sin Qd} \xi_n + O(\epsilon_n^2, \xi_n^2). \end{aligned} \quad (16)$$

The error term in equation (16) means all quadratic (or higher-order) combinations of ϵ_n and ξ_n .

2.3 Derivation of the dispersion relation for the perturbed phononic crystal

We now adapt the CPA when the host medium corresponds to a periodic-on-average medium. Here, the characteristics of the cells forming the host medium result from an average (of its position and scattering strength).

We thus impose the vanishing of the scattering matrix on average

$$\langle t \rangle = 1 \quad \text{and} \quad \langle r \rangle = 0, \quad (17)$$

where we define averaging by

$$\langle f \rangle = \frac{1}{\epsilon\xi} \int_{-\epsilon/2}^{\epsilon/2} \int_{-\xi/2}^{\xi/2} f(\epsilon_n, \xi_n) d\xi_n d\epsilon_n.$$

Although it would be possible to deal with the explicit expressions of t and r , it turns out that it is more convenient to average the system (10). Thus, using equation (17), we obtain

$$\begin{cases} 1 + iV(1 + t_\xi) - e^{i(k-K)d} + iV(t_\epsilon + t_{\epsilon\xi})\mathcal{B} = 0, \\ -iV(t_\epsilon + t_{\epsilon\xi}) + (1 - iV(1 + t_\xi) - e^{-i(k+K)d})\mathcal{B} = 0, \end{cases} \quad (18)$$

where we have defined the unknown averaged quantities

$$\begin{cases} t_\xi \equiv \langle t_{\xi_n} \rangle, \\ t_\epsilon \equiv \langle t_{\epsilon_n} e^{\pm 2i\epsilon_n kd} \rangle, \\ t_{\epsilon\xi} \equiv \langle t_{\xi_n} e^{\pm 2i\epsilon_n kd} \rangle. \end{cases} \quad (19)$$

As in the periodic case, we obtain the dispersion relation by eliminating \mathcal{B} in equation (18). The Floquet wavenumber K satisfies

$$\cos Kd = \cos Qd + Vt_\xi \sin kd - V^2 e^{iKd} \mathcal{T}_1, \quad (20)$$

where we have used equation (14) and we have defined

$$\mathcal{T}_1 \equiv \frac{1}{2} [(1 + t_\xi)^2 - (t_\epsilon + t_{\epsilon\xi})^2]. \quad (21)$$

We can also calculate \mathcal{B} from equation (18),

$$\mathcal{B} = \frac{e^{i(k-K)d} - 1 - iV\mathcal{T}_2}{1 - e^{-i(k+K)d} - iV\mathcal{T}_2}, \quad (22)$$

with

$$\mathcal{T}_2 \equiv 1 - t_\epsilon + t_\xi - t_{\epsilon\xi}. \quad (23)$$

At this stage, we have not made any approximations. However, the characteristics of the normal Floquet mode require that \mathcal{T}_1 and \mathcal{T}_2 (defined in Eqs. (21) and (23)) be determined, and these quantities depend on the value of t , which is unknown. Thus, we derive an expression for t , obtained assuming that ϵ and ξ are small. To obtain a second-order approximation to equations (20) and (22), we see that we need only a linear approximation for t . This is obvious from equation (19) for t_ξ and $t_{\epsilon\xi}$; for t_ϵ , it is sufficient to remark that $t_\epsilon = 1 - 2\langle t \sin^2(\epsilon_n kd) \rangle$, and $\sin^2(\epsilon_n kd)$ is a second-order term in ϵ_n . The expansion of t is

$$\begin{aligned} t(\epsilon, \xi; \epsilon_n, \xi_n) &= a_0 + a_1\epsilon + b_1\xi + c_1\xi_n \\ &+ O(\epsilon_n^2, \xi_n^2, \xi^2, \epsilon^2); \end{aligned} \quad (24)$$

there is no term linear in ϵ_n since equation (11) shows that t is an even function of ϵ_n .

We now derive the coefficients a_0 , a_1 , b_1 and c_1 in the expansion (24). We first use that $t(0, 0; \epsilon_n, \xi_n) = t_0(\epsilon_n, \xi_n)$ and then from equation (16) we obtain

$$a_0 = 1, \quad c_1 = -iV \frac{\sin kd}{\sin Qd}. \quad (25)$$

Then, using $\langle t \rangle = 1$ in equation (24), namely $\langle t \rangle = 1 + a_1\epsilon + b_1\xi$ (since $\langle \xi_n \rangle = 0$), gives

$$a_1 = b_1 = 0.$$

Thus, correct to first order,

$$t = 1 - iV \frac{\sin kd}{\sin Qd} \xi_n + O(\epsilon_n^2, \xi_n^2, \xi^2, \epsilon^2).$$

The averages t_ξ , t_ϵ and $t_{\epsilon\xi}$ in equations (19) are

$$\begin{aligned} t_\xi &= -\frac{iV \sin kd}{12 \sin Qd} \xi^2 + O(\xi^3, \epsilon^3), \\ t_\epsilon &= \text{sinc}(\epsilon kd) + O(\xi^4, \epsilon^4), \\ t_{\epsilon\xi} &= t_\xi + O(\xi^3, \epsilon^3), \end{aligned}$$

with $\text{sinc } x = (\sin x)/x$. Then, from equations (21) and (23), we deduce that

$$\mathcal{T}_1 = 1 - \text{sinc}(\epsilon kd) + O(\xi^3, \epsilon^3) = \mathcal{T}_2. \quad (26)$$

Hence the dispersion relation (20) becomes

$$\begin{aligned} \cos Kd &= \cos Qd - V^2 [1 - \text{sinc}(\epsilon kd)] e^{iKd} \\ &- i \frac{V^2 \sin^2 kd}{12 \sin Qd} \xi^2 + O(\xi^3, \epsilon^3), \end{aligned} \quad (27)$$

and the function f is defined with \mathcal{B}

$$\mathcal{B} = \frac{e^{i(k-K)d} - 1 - iV[1 - \text{sinc}(\epsilon kd)]}{1 - e^{-i(k+K)d} - iV[1 - \text{sinc}(\epsilon kd)]} + O(\xi^3, \epsilon^3). \quad (28)$$

Obviously, in the absence of disorder ($\epsilon = \xi = 0$), we recover that $K = Q$ in (27) and $\mathcal{B} = \mathcal{B}_0$ in (28).

2.4 Remarks on the effective wavenumber

Our expressions for K (Eq. (27)), diverge at the band edges of the underlying periodic medium, where $\sin Qd = 0$. This happens when $\cos k_d d + V \sin k_d d = \pm 1$ for some non-zero $\sin k_d d$. In acoustics, with a potential $V \propto k$, the low-frequency regime corresponds to a pass band with the first band edge at $kd = \pi$. The first stop band appears for $\pi < kd < k_d d$, with $k_d d$ a band edge depending on V . Thus, we expect our expressions to be valid below the second band edge, or away from the band edges.

As we expect K to be close to Q , equation (27) can be written

$$Kd \simeq Qd + \frac{V^2 (kd)^2 e^{iQd}}{6 \sin Qd} \epsilon^2 + i \frac{V^2 \sin^2 kd}{12 \sin^2 Qd} \xi^2. \quad (29)$$

In a pass band, Q is real and then equation (29) gives

$$\text{Re}(Kd) = Qd + \frac{V^2(kd)^2}{6 \tan Qd} \epsilon^2, \quad (30)$$

with no contribution from the compositional disorder. Taking the imaginary part of equation (29) gives

$$\text{Im}(Kd) = \frac{V^2}{6} \left[(kd)^2 \epsilon^2 + \frac{\sin^2 kd}{2 \sin^2 Qd} \xi^2 \right]. \quad (31)$$

Thus, in a pass band, both kinds of disorder create an attenuation.

In a stop band, Q is imaginary and equation (29) yields $\text{Re}(Kd) = 0$ and

$$\text{Im}(Kd) = \text{Im}(Qd) + \frac{V^2}{6} \left[\frac{(kd)^2 e^{iQd}}{\sinh(iQd)} \epsilon^2 + \frac{\sin^2 kd}{2 \sin^2 Qd} \xi^2 \right]. \quad (32)$$

Again, both kinds of disorder create an attenuation.

The imaginary part of K is equivalent to the inverse of the localization length L_{loc}^{-1} , as calculated in [19] using a Hamiltonian map approach appropriate for deriving the Lyapunov exponent in an infinite system (to our knowledge, this is the only approach able to deal with infinite systems). Specifically, equation (8.37) in reference [19] gives the localization length in the form

$$\frac{d}{L_{\text{loc}}} = \frac{V^2}{2} \left[\frac{\sin^2 kd}{\sin^2 Qd} \langle \xi_n^2 \rangle + \frac{k^2}{\sin^2 Qd} \langle \Delta_n^2 \rangle \mathcal{K}_\Delta \right]. \quad (33)$$

Here, Δ_n is defined as the perturbation in the distance between scatterers, $x_{n+1} - x_n = d + \Delta_n$, and it is assumed to satisfy $k^2 \langle \Delta_n^2 \rangle \ll 1$. The function \mathcal{K}_Δ refers to possible correlations; for two-point correlation, we have

$$\mathcal{K}_\Delta = 1 + 2 \frac{\langle \Delta_n \Delta_{n+1} \rangle}{\langle \Delta_n^2 \rangle} \cos 2Qd. \quad (34)$$

Our definition of ϵ_n concerns the disorder in the position of the scatterers rather than from their relative distance Δ_n . In the absence of correlation, the probability distribution of the distance between nearest scatterers is constant while in our case, it is a triangular distribution with maximum probability at d and with a length that is a measure of the ϵ value [25]. The link between Δ_n and ϵ_n is

$$\Delta_n = d(\epsilon_{n+1} - \epsilon_n) \quad (35)$$

from which we deduce $\langle \Delta_n^2 \rangle = 2d^2 \langle \epsilon_n^2 \rangle$ and $\mathcal{K}_\Delta = 2 \sin^2 Qd$. Substituting in equation (33), using $\langle \epsilon_n^2 \rangle = \epsilon^2/12$ and $\langle \xi_n^2 \rangle = \xi^2/12$, gives

$$\frac{d}{L_{\text{loc}}} = \frac{V^2}{6} \left[(kd)^2 \epsilon^2 + \frac{\sin^2 kd}{4 \sin^2 Qd} \xi^2 \right], \quad (36)$$

which should be compared with equation (31). Thus, it appears that our attenuation length $\text{Im}(Kd)$ coincides with the localization length as proposed in [19] in the limit $\epsilon kd \ll 1$ for the positional disorder but differs for the compositional disorder by an additional factor 2. We do not have an explanation for this discrepancy.

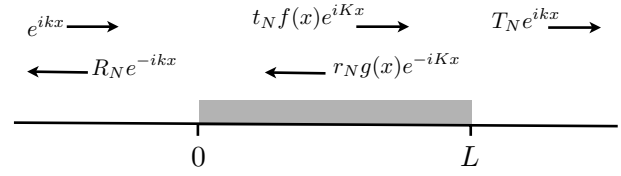


Fig. 2. Reflection and transmission of a wave incident in free space by a slab made of an effective medium periodic on average; the slab has finite size L .

2.5 Transmission amplitude through a slab of finite size

Until now, we have considered the effective medium occupying the whole space from $x \rightarrow -\infty$ to $x \rightarrow \infty$. We now focus on a slab of effective medium occupying a finite region of space, $0 \leq x \leq L$ (Fig. 2). An incident wave e^{ikx} in free space is partly reflected and partly transmitted by the slab. The reflection and transmission amplitudes, R_N and T_N , are determined by applying the continuity conditions of the field v_N and its first derivative across the two interfaces $x = 0, L$, with

$$v_N(x) = \begin{cases} e^{ikx} + R_N e^{-ikx}, & x \leq 0, \\ t_N f(x) e^{iKx} + r_N g(x) e^{-iKx}, & 0 \leq x \leq L, \\ T_N e^{ikx}, & x \geq L, \end{cases}$$

f, g and K being known from equations (9), (27) and (28). It directly follows that

$$T_N = e^{-ikNd} \frac{e^{ikd} - \mathcal{B}^2 e^{-ikd}}{e^{ikd-iKNd} - \mathcal{B}^2 e^{-ikd+iKNd}}. \quad (37)$$

This expression for the transmission amplitude accounts for all the internal reflections inside the slab. This is because the complete normal forms of the Floquet modes have been determined. In the absence of disorder, $\epsilon = \xi = 0$, the expression for T_N is exact (with $K = Q$ and $\mathcal{B} = \mathcal{B}_0$). When disorder is present, we have assumed that a slab of finite size made of the perturbed periodic medium behaves as a slab of the same size but made of the effective medium. This means that we neglect possible boundary effects near $x = 0$ and $x = L$. This point will be discussed elsewhere.

3 Results

3.1 Numerical implementation

Direct numerical calculations of the exact wavefields $u(x)$ with N scatterers were performed. A configuration consists of N scatterers located at $x_n = (n + \epsilon_n)d$, with strength $V_n = V(1 + \xi_n)$, $n = 0, 1, \dots, N - 1$, ϵ_n and ξ_n being randomly chosen with $|\epsilon_n| < \epsilon/2$ and $|\xi_n| < \xi/2$ (Fig. 3). An average of N_{real} realizations of disordered configurations is then performed to get $v(x) \equiv \langle u \rangle(x)$.

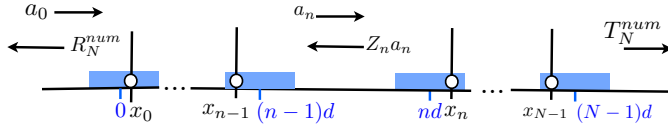


Fig. 3. Convention used in the direct numerical calculations using the impedance method (Z_n).

To calculate $u(x)$, we avoid implementing the transfer matrix method. Indeed, although the transfer matrix approach is applicable in principle, numerical algorithms suffer from instabilities [26]. Rather, we implement a method based on the impedance (denoted Z_n) [27,28], similar to reflection or scattering matrix methods [29].

In each cell, $x_{n-1} \leq x \leq x_n$, the wavefield can be written

$$u(x) = a_n \left[e^{ik(x-x_n)} + Z_n e^{-ik(x-x_n)} \right], \quad (38)$$

where Z_n is the impedance (equivalent to the Dirichlet-to-Neumann operator). The impedance is initiated with $Z_N = 0$, which accounts for the radiation condition after the N th scatterer. Then, at each scatterer, the conditions $[u]_{x_n} = 0$ and $[u']_{x_n} = 2kV_n u(x_n)$ give a backward-recurrence relation for Z_n ,

$$Z_n = \frac{-iV_n e^{-i\varphi_n} + Z_{n+1}(1 - iV_n)e^{i\varphi_n}}{(1 + iV_n)e^{-i\varphi_n} + iZ_{n+1}V_n e^{i\varphi_n}}, \quad (39)$$

with $\varphi_n \equiv k(x_{n+1} - x_n)$, and $\varphi_N = 0$ (for convenience, a ghost scatterer has been added at $x_N = x_{N-1}$). Once $(Z_n)_{n=0,1,\dots,N}$ have been computed, the amplitudes $(a_n)_{n=0,1,\dots,N}$ are derived accounting for the source $a_0 = e^{ikx_0}$ and using the forward-recurrence

$$a_{n+1} = (1 - iV_n Z_n - iV_n) e^{i\varphi_n} a_n. \quad (40)$$

The reflection and transmission amplitudes are deduced for each realization i , $1 \leq i \leq N_{real}$,

$$R_{N,i}^{num} = Z_0 e^{2ikx_0}, \quad T_{N,i}^{num} = Z_N e^{-ikx_N}, \quad (41)$$

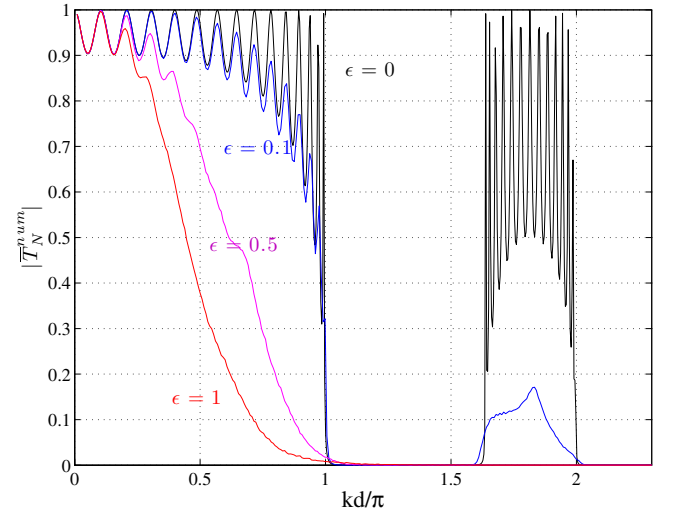
followed by an averaging over all realizations,

$$R_N^{num} = \frac{1}{N_{real}} \sum_i R_{N,i}^{num}, \quad T_N^{num} = \frac{1}{N_{real}} \sum_i T_{N,i}^{num}. \quad (42)$$

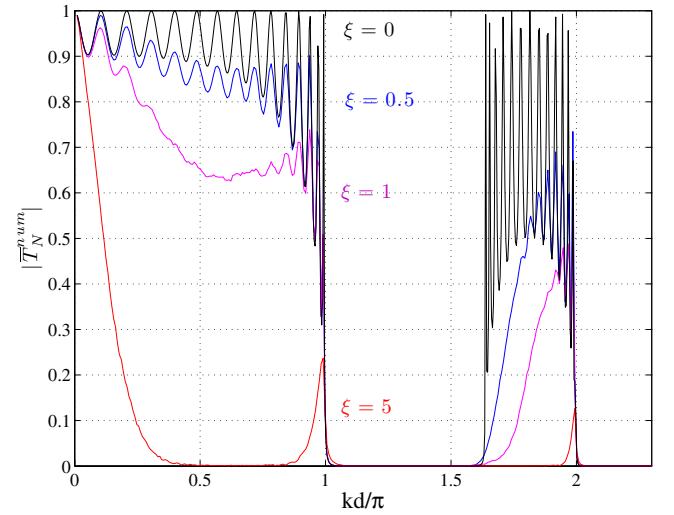
Results presented in this section have been obtained considering $V = 0.3k$ (in the acoustic case, the potential $2kV_n$ in Eq. (1) is proportional to k^2).

3.2 Numerical results

Figure 4 shows $|T_N^{num}|$ computed numerically ($N_{real} = 10^4$ averages have been performed) for a slab of length $N = 15$. We observe a clear difference in the resulting extinction spectra and transmission spectra. In the case of positional disorder, increasing the disorder makes the transmission vanish except in the low frequency regime. This includes



(a)



(b)

Fig. 4. Converged numerical values of $|T_N|$ as a function of the frequency for (a) various amounts of disorder in position ϵ ($\epsilon = 0, 0.1, 0.5$ and 1) and (b) various amounts of disorder in strength $\xi = 0, 0.5, 1$ and 5 .

the gradual disappearance of the pass bands. For the maximum value of disorder, $\epsilon = 1$, the phononic crystal has almost completely lost its band structure. Remarkably, this also means that the introduced disorder can produce an increase in the attenuation length that is a delocalization in the stop band of the perfect phononic crystal (the transmission increases from $\epsilon = 0$ to $\epsilon = 1$ for $kd \in [1, 1.6]\pi$). In the presented case, this mechanism is less impressive than the one presented in [10] where a stop band was found to become an almost perfect pass band.

In the case of compositional disorder, increasing the disorder produces also a global decrease in the transmission. However, because the phononic crystal keeps its spatial periodicity, the Bragg resonances at $kd = n\pi$ are still efficient, resulting in a conflict between disorder-induced localization and periodicity-induced constructive

interferences at those frequencies. A similar conflict has been observed in [30] for scatterers made of alternating dielectric slabs with positional disorder; in that case, the survival of the Fabry-Perot resonant bands inside the slabs of constant length was responsible for the observed delocalization.

The second band edge at k_0d with $\cos k_0d + V \sin k_0d = -1$ (here around 1.6π), being sensitive to the value of the potential at each scatterer, disappears when the disorder in potential increases. It results in the collapse of a pass band and a stop band where the localization increases in between two delocalized states at $kd = n\pi$ and $kd = (n+1)\pi$.

3.3 Comparison with CPA approach

Here, the results from direct numerical computation of the transmission amplitude are compared with the transmission amplitude $|T_N|_{CPA}$ in equation (37),

$$|T_N|_{CPA} = \left| \frac{e^{ikd} - \mathcal{B}^2 e^{-ikd}}{e^{ikd-iKNd} - \mathcal{B}^2 e^{-ikd+iKNd}} \right|, \quad (43)$$

with K in equation (20) and \mathcal{B} in equation (27). In addition, we report a comparison with a quantity often used in localization studies,

$$|T_N|_{loc} \equiv e^{-Nd/L_{loc}}, \quad (44)$$

with $d/L_{loc} = \text{Im}(Kd)$ in equation (27). It is known that this quantity is questionable depending on whether the system is in the localization regime or in the ballistic regime (for a discussion see, e.g., [19]). However, it has been shown in a series of papers that, for random systems that are periodic on average, this analytical expression for the transmission coefficient reproduces quite well the frequency dependence of the transmission spectra [30–32], and it is often referred as the “localization factor” in this literature.

Results are shown on Figures 5 and 6 for $kd \leq 1.5\pi$. For large positional disorder, we see the expected difficulties near band edges (appearing in Eq. (27) when $\sin Qd = 0$ and $\sin kd \neq 0$). These regions require special treatment [19,33]. Except in those regions, we observe that the transmission properties of the perturbed periodic medium are captured reasonably well by $|T_N|_{loc}$. However, because it disregards the finite size effects of the slab, it is less accurate than our prediction from the CPA approach, $|T_N|_{CPA}$. To obtain this accuracy, the Bloch-Floquet mode has to be fully characterized, beyond the determination of the effective wavenumber only.

To quantify further the accuracy of both predictions, we report in Figure 7 the error between the predictions and the computed transmission as a function of the disorder strength and as a function of the frequency. Clearly, $|T_N|_{loc}$ is unable to quantitatively evaluate $|T_N|$, which can be seen as problematic if inverse problems are to be contemplated. This is because the small error due to the

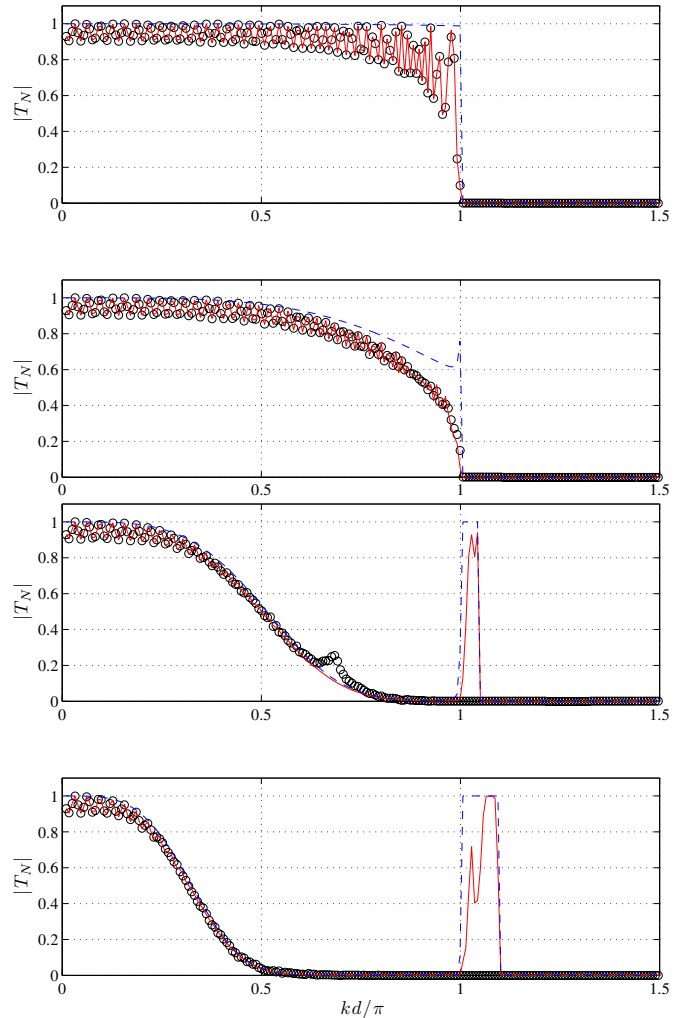


Fig. 5. Transmission $|T_N|$ as a function of kd/π in a slab of length $N = 50$ for increasing ϵ , from top to bottom $\epsilon = 0.1, 0.14, 0.34$ and 1 . Black symbols show numerical calculations with $N_{real} = 10^3$ ensemble averages, plain red lines show $|T_N|_{CPA}$ from (37) and dotted blue lines show $|T_N|_{loc} = e^{-Nd/L_{loc}}$, with $1/L_{loc} = \text{Im}(Kd)$ in (27).

omission of the internal reflections can be of the same order as the – also small – effect of the disorder that one wants to capture.

4 Concluding remarks

We have presented a full characterization of the Bloch-Floquet mode of the periodic-on-average medium resulting from a one-dimensional crystal perturbed in both position and potential strength. Assuming that the characteristics of this mode are still valid when considering a slab of finite size, the transmission amplitude has been obtained. The localization factor is an estimate of the transmission amplitude based on the localization length, which disregards the finite length of the slab. It is a good indicator

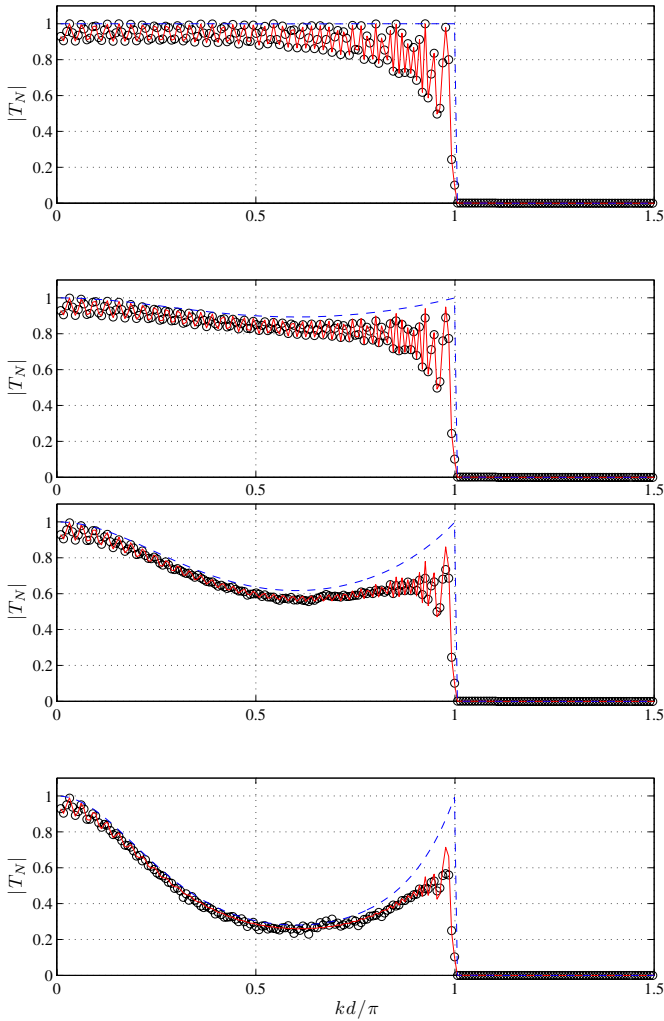


Fig. 6. Same representation as in Figure 5 for increasing ξ , from top to bottom $\xi = 0.01, 0.3, 0.6$ and 1 .

of the effect of disorder but it is quantitatively unable to reproduce the effect of the disorder. The CPA approach gives a prediction of $|T_N|$ that accounts for the oscillations of $|T_N|$ due to internal reflections, and it is well adapted to describe quantitatively the scattering properties of real systems. It is of interest to consider related inverse problems, inferring disorder properties from transmission measurements, for example.

One of the authors (AM) acknowledges the financial support of the Agence Nationale de la Recherche through the Grant ANR ProCoMedia, Project ANR-10-INTB-0914.

Appendix: Derivation of the scattering matrix

The scattering matrix can be easily calculated owing to the form of f in equation (9) and owing to the form of the

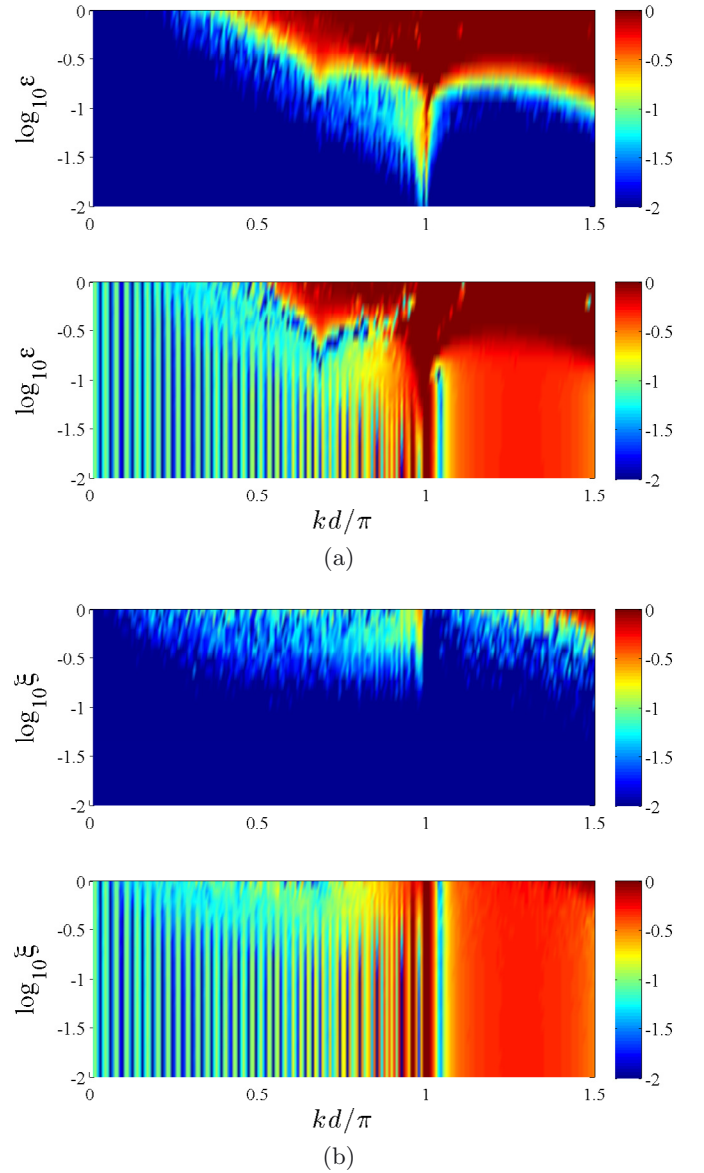


Fig. 7. Errors in the $|T_N|$ estimate as a function of the disorder strength and as a function of kd . (a) For positional disorder ϵ and (b) for compositional disorder ξ . The plots on the top show the error $|T_N| - |T_N|_{\text{CPA}}$ normalized with $|T_N|$. The bottom plots show the error $|T_N| - |T_N|_{\text{loc}}$.

transfer matrices defined as:

$$\begin{pmatrix} A_1 e^{iknd} \\ B_1 e^{-iknd} \end{pmatrix} = \mathsf{T}_1 \begin{pmatrix} a_1 e^{iKnd} \\ b_1 e^{-iKnd} \end{pmatrix} \quad (\text{A.1})$$

$$\begin{pmatrix} A_2 e^{iknd} \\ B_2 e^{-iknd} \end{pmatrix} = \mathsf{T}_s \begin{pmatrix} A_1 e^{iknd} \\ B_1 e^{-iknd} \end{pmatrix} \quad (\text{A.2})$$

$$\begin{pmatrix} a_2 e^{iKnd} \\ b_2 e^{-iKnd} \end{pmatrix} = \mathsf{T}_2 \begin{pmatrix} A_2 e^{iknd} \\ B_2 e^{-iknd} \end{pmatrix}. \quad (\text{A.3})$$

The continuity conditions for v and v' are applied at the interfaces $(n-1)d + y$ and $nd + y$. At the scatterer position

$x = x_n$, v satisfies $v(x_n^-) = v(x_n^+)$ and $v'(x_n^+) - v'(x_n^-) = 2kV_nv(x_n)$, with $V_n = V(1 + \xi_n)$. We deduce

$$\mathbb{T}_1 = \begin{pmatrix} e^{i(k-K)d} & \mathcal{B} \\ \mathcal{B}e^{-i(K+k)d} & 1 \end{pmatrix} \quad (\text{A.4})$$

$$\mathbb{T}_s = \begin{pmatrix} (1 - iV_n) & -iV_ne^{-2i\epsilon_n d} \\ iV_ne^{2i\epsilon_n d} & (1 + iV_n) \end{pmatrix} \quad (\text{A.5})$$

and

$$\mathbb{T}_2 = \frac{e^{i(k-K)d}}{1 - \mathcal{B}^2 e^{-2ikd}} \begin{pmatrix} e^{i(k-K)d} & -\mathcal{B}e^{-i(k+K)d} \\ -\mathcal{B} & 1 \end{pmatrix}. \quad (\text{A.6})$$

The total scattering matrix is deduced from the transfer matrix \mathbb{T} ,

$$\begin{pmatrix} a_2 e^{iKnd} \\ b_2 e^{-iKnd} \end{pmatrix} = \mathbb{T} \begin{pmatrix} a_1 e^{iKnd} \\ b_1 e^{-iKnd} \end{pmatrix} \quad (\text{A.7})$$

and

$$\mathbb{T} = \begin{pmatrix} T_{11} & T_{12} \\ T_{21} & T_{22} \end{pmatrix} \quad (\text{A.8})$$

with

$$T_{11} = \frac{e^{-i(K+k)d}}{1 - \mathcal{B}^2 e^{-2ikd}} \left[(1 - iV_n)e^{2ikd} - 2iV_n\mathcal{B} \cos(2\epsilon_n kd) - (1 + iV_n)\mathcal{B}^2 e^{-2ikd} \right],$$

$$T_{22} = \frac{e^{i(K-k)d}}{1 - \mathcal{B}^2 e^{-2ikd}} \left[(1 + iV_n) + 2iV_n\mathcal{B} \cos(2\epsilon_n kd) - (1 - iV_n)\mathcal{B}^2 \right],$$

$$T_{12} = \frac{e^{-ikd}}{1 - \mathcal{B}^2 e^{-2ikd}} \left[-iV_n \left(e^{ikd(1-2\epsilon)} + \mathcal{B}^2 e^{-ikd(1-2\epsilon)} \right) + 2i\mathcal{B}(\sin kd - V_n \cos kd) \right],$$

$$T_{21} = \frac{e^{-ikd}}{1 - \mathcal{B}^2 e^{-2ikd}} \left[iV_n \left(e^{ikd(1+2\epsilon)} + \mathcal{B}^2 e^{-ikd(1+2\epsilon)} \right) - 2i\mathcal{B}(\sin kd - V_n \cos kd) \right],$$

gives the scattering matrix, defined by

$$\begin{pmatrix} b_1 \\ a_2 \end{pmatrix} = \mathbb{S} \begin{pmatrix} a_1 \\ b_2 \end{pmatrix} \quad (\text{A.9})$$

with

$$\mathbb{S} = \begin{pmatrix} r & \tilde{t} \\ t & \tilde{r} \end{pmatrix} \quad (\text{A.10})$$

and

$$r = -\frac{T_{21}}{T_{22}} e^{2iKnd}, \quad t = \frac{1}{T_{22}},$$

$$\tilde{r} = -\frac{T_{12}}{T_{22}} e^{-2iKnd}, \quad \tilde{t} = \frac{1}{T_{22}},$$

where we have used $T_{11}T_{22} - T_{12}T_{21} = 1$. Explicit expressions for r , \tilde{r} , t and \tilde{t} can be obtained. Rather than give these, we give the pairs (r, t) and (\tilde{r}, \tilde{t}) as the solutions of two systems of coupled equations

$$\begin{cases} [1 + iV_n + iV_n\mathcal{B}e^{-2i\epsilon_n kd}]t - \mathcal{B}re^{-2iKnd} = e^{i(k-K)d}, \\ [-iV_ne^{2i\epsilon_n kd} + \mathcal{B}(1 - iV_n)]t - re^{-2iKnd} = \mathcal{B}e^{-i(k+K)d}, \end{cases} \quad (\text{A.11})$$

and

$$\begin{cases} [1 + iV_n + iV_n\mathcal{B}e^{2i\epsilon_n kd}]\tilde{t} + \mathcal{B}\tilde{r}e^{2iKnd} = e^{i(k-K)d}, \\ [-iV_ne^{-2i\epsilon_n kd} + \mathcal{B}(1 - iV_n)]\tilde{t} + \tilde{r}e^{2iKnd} = \mathcal{B}e^{-i(k+K)d}. \end{cases} \quad (\text{A.12})$$

References

1. C. Qiu, Z. Liu, J. Mei, J. Shi, Appl. Phys. Lett. **87**, 104101 (2005)
2. V. Romero-Garcia, C. Lagarrigue, J.-P. Groby, O. Richoux, V. Tournat, J. Phys. D **46**, 305108 (2013)
3. M.I. Hussein, K. Hamza, G.M. Hulbert, K. Saitou, Waves in Random and Complex Media **17**, 491 (2007)
4. T.Z. Wu, S.T. Chen, IEEE Trans. Microwave Th. and Tech. **54**, 3398 (2006)
5. J.H. Page, A. Sukhovich, S. Yang, M.L. Cowan, F. Van Der Biest, A. Tourin, M. Fink, Z. Liu, C.T. Chan, P. Sheng, Phys. Stat. Sol. B **241**, 3454 (2004)
6. S. John, Phys. Today **44**, 32 (1991)
7. A.R. McGurn, K.T. Christensen, F.M. Mueller, A.A. Maradudin, Phys. Rev. B **47**, 120 (1993)
8. A.A. Asatryan, L.C. Botten, M.A. Byrne, V.D. Freilikher, S.A. Gredeskul, I.V. Shadrivov, R.C. McPhedran, Y.S. Kivshar, Phys. Rev. Lett. **99**, 193902 (2007)
9. A. Maurel, A. Ourir, J.-F. Mercier, V. Pagneux, Phys. Rev. B **85**, 205138 (2012)
10. A.N. Poddubny, M.V. Rybin, M.F. Limonov, Y.S. Kivshar, Nat. Commun. **3**, 914 (2012)
11. R. de L. Kronig, W.G. Penney, Proc. R. Soc. Lond. A **130**, 499 (1931)
12. H. Levine, *Unidirectional Wave Motions* (North-Holland, Amsterdam, 1978)
13. O. Richoux, V. Pagneux, Europhys. Lett. **59**, 34 (2002)
14. O. Richoux, V. Tournat, T. Le Van Suu, Phys. Rev. E **75**, 026615 (2007)
15. U. Kuhl, H.-J. Stöckmann, Phys. Rev. Lett. **80**, 3232 (1998)
16. U. Kuhl, F.M. Izrailev, A.A. Krokhin, Phys. Rev. Lett. **100**, 126402 (2008)
17. A. Mayer, Phys. Rev. E **74**, 046708 (2006)
18. D.R. Nacbar, A. Bruno-Alfonso, Phys. Rev. B **85**, 195127 (2012)
19. F.M. Izrailev, A.A. Krokhin, N.M. Makarov, Phys. Rep. **512**, 125 (2012)
20. J.M. Ziman, *Models of Disorder* (Cambridge University Press, Cambridge, 1979)
21. A. Maurel, P.A. Martin, V. Pagneux, Waves in Random and Complex Media **20**, 634 (2010)
22. R.-L. Chern, D. Felbacq, Phys. Rev. B **80**, 205115 (2009)
23. X. Hu, C.T. Chan, Phys. Rev. Lett. **95**, 154501 (2005)

24. D. Torrent, A. Hakansson, F. Cervera, J. Sanchez-Dehesa, Phys. Rev. Lett. **96**, 204302 (2006)
25. A. Maurel, V. Pagneux, Phys. Rev. B **78**, 052301 (2008)
26. J.W. Dunkin, Bull. Seismol. Soc. Am. **55**, 335 (1965)
27. V. Pagneux, N. Amir, J. Kergomard, J. Acoust. Soc. Am. **100**, 2034 (1996)
28. V. Pagneux, A. Maurel, Proc. R. Soc. Lond. A **458**, 1913 (2002)
29. L. Li, J. Opt. Soc. Am. A **13**, 1024 (1996)
30. G.A. Luna-Acosta, F.M. Izrailev, N.M. Makarov, U. Kuhl, H.-J. Stöckmann, Phys. Rev. B **80**, 115112 (2009)
31. Y. Pang, Y.-S. Wang, J.-X. Liu and D.-N. Fang, Smart Mater. Struct. **19**, 055012 (2010)
32. Z.-Z. Yan, C. Zhang, Y.-S. Wang, Wave Motion **47**, 409 (2010)
33. L.I. Deych, A.A. Lisyansky, B.L. Altshuler, Phys. Rev. Lett. **84**, 2678 (2000)